Requirement for Natively Unstructured Regions of Mesoderm Development Candidate 2 in Promoting Low-Density Lipoprotein Receptor-Related Protein 6 Maturation†

Vidyasagar Koduri and Stephen C. Blacklow*

Department of Pathology, Brigham and Women's Hospital and Harvard Medical School, Boston, Massachusetts 02115

Received January 11, 2007; Revised Manuscript Received March 4, 2007

ABSTRACT: Proteins of the low-density lipoprotein receptor family (LRPs) are complex, multimodular type I transmembrane receptors. Productive maturation of these proteins relies on an ER-resident protein called mesoderm development candidate 2 (MESD) in mammals and Boca in *Drosophila*. We show here that MESD contains a central folded domain flanked by natively unstructured regions required to facilitate maturation of LRP6. Enforced expression of full-length human MESD promotes the secretion of soluble minireceptors derived from LRP6 that contain either one or two β-propeller−EGF domain pairs. Conversely, siRNA-mediated knockdown of human MESD expression blocks secretion of native LRP6 minireceptors and dramatically reduces the level of cell-surface expression of full-length LRP6. Cell-surface expression is only rescued by simultaneous delivery of siRNA-resistant forms of mouse MESD that contain most or all of the unstructured N- and C-termini, implicating the flexible parts of MESD in its function of promoting LRP maturation.

Wnts are a family of extracellular proteins that play important roles in both embryonic development and adult metabolic homeostasis. Wnts are recognized by members of the Frizzled family of transmembrane receptors; the different Wnts bind in a well-defined manner to their cognate Frizzled receptors (*1*). A wealth of genetic and biochemical evidence shows that signaling by certain Wnts requires the LDL[1] receptor-related protein 6 (LRP6) (*2*, *3*); indeed, some Wnts appear to drive formation of a ternary complex between Frizzled (Fz), Wnt, and LRP6 (*4*). In the absence of Wnt stimulation, the axin−APC−GSK3β complex mediates the phosphorylation and destruction of β-catenin. In canonical Wnt signaling, the formation of the LRP6−Fz−Wnt ternary complex leads to the destruction of the axin−APC−GSK3β scaffold and an accompanying increase in β-catenin levels, which in turn drive the transcription of target genes (*5*).

LRP6 is a large (1613 residue) modular type I transmembrane protein of the low-density lipoprotein receptor family (*6*). The mature protein has an extracellular region that consists of a series of four propeller−EGF domain pairs, followed by three LDL-A repeats, a transmembrane domain, and a cytoplasmic tail (*6*). The different propeller−EGF pairs appear to act as distinct functional units by binding different protein ligands; deletion studies implicate the two N-terminal propeller−EGF pairs in Wnt recognition (*7*), while the two C-terminal pairs participate in the recognition of Dickkopf-1 (*8*).

Productive maturation of the LDL receptor-related Wnt coreceptors LRP5 and LRP6 relies on an ER-resident protein called MESD in mouse and Boca in *Drosophila* (*9*, *10*). Mice lacking MESD die in utero with a phenotype that resembles that of the Wnt3 knockout, while flies lacking Boca have an embryonic lethal phenotype that resembles loss of function of Arrow, the *Drosophila* homologue of LRP6.

Studies of Boca using both loss- and gain-of-function approaches argue that Boca promotes the cell-surface expression of proteins containing YWTD β-propeller domains that are followed by EGF-like repeats (*9*, *11*). These studies suggest that Boca may bind directly to the β-propeller domain via an interaction suppressed when the adjacent C-terminal EGF repeat is also present. The introduction of space-filling mutations (W → K) that disturb the presumed β-propeller−EGF repeat interdomain interface allows co-immunoprecipitation of certain propeller−EGF domain pairs with Boca after reversible cross-linking. In contrast, the YWTD propeller of Sevenless, which occurs in isolation without an EGF domain, is secreted in S2 cells in a Boca-independent manner, consistent with the notion that Boca binds selectively to propeller domains that normally pack against EGF repeats when folded.

In the case of MESD, previous investigations using molecular and cell-based assays have been limited to enforced expression approaches. These studies have shown that expression of LRP6 without concomitant expression of MESD accumulates in disulfide-linked aggregates that are

† This work was supported by grants from the NIH (HL61001 to S.C.B.) and the American Heart Association (to S.C.B.).

* To whom correspondence should be addressed. Tel: (617) 525-4415. Fax: (617) 525-4414. E-mail: sblacklow@rics.bwh.harvard.edu.

[1] Abbreviations: APC, ademnoatous polyposis coli; CD, circular dichroism; DTT, dithiothreitol; EGF, epidermal growth factor; ER, endoplasmic reticulum; HA, hemagluttinin; HUVEC, human umbilical vein endothelial cells; GFP, green fluorescent protein; IPTG, isopropyl β-D-thiogalactopyranoside; LDL, low-density lipoprotein; LRP, low-density lipoprotein receptor-related protein; GSK, glycogen synthase kinase; MESD, mesoderm development candidate 2; NTA, nitrilotriacetic acid; PCR, polymerase chain reaction; VSV, vesicular stomatitis virus.

10.1021/bi700049g CCC: $37.00 © 2007 American Chemical Society
Published on Web 05/09/2007

largely intracellular. Cotransfection of MESD in mammalian cells appears to decrease the accumulation of disulfide-linked aggregates, decrease the fraction of LRP6 trapped within the cell, and increase the fraction of LRP6 at the cell surface (*10*). Co-immunoprecipitation studies suggest that MESD can associate with both LRP5 and LRP6, with a binding site on LRP5 mapped to the first two propeller−EGF pairs (*12*).

Though these studies implicate MESD in the productive maturation of the Wnt coreceptors LRP5 and LRP6, a more extensive analysis of MESD structure−function relationships in the maturation of LRP6 has not yet been reported. In these studies, we first establish that MESD consists of a core folded domain flanked by N- and C-terminal regions with conformational flexibility. Then, we show in rescue experiments following siRNA-mediated loss of function that the flexible regions at the N- and C-termini of MESD are required for productive function as a maturation factor in the export of LRP6. The conformational flexibility of the termini of MESD may thus be important for its role in promoting the maturation of a family of similar, but nonidentical, substrate receptors.

MATERIALS AND METHODS

Cloning of Propeller−EGF Domains of LRP6 and Murine MESD Constructs. VSV-G-tagged LRP6 (p520) was the kind gift of X. He. A multiple sequence alignment of the predicted propeller−EGF domains against other YWTD propeller−EGF domains was used to identify the precise start and end points of the four propeller−EGF domains (*13*). Using p520 as a template, we cloned a number of domains from LRP6 into pcDNA3.1+ (Invitrogen). The nomenclature and domain organization of these constructs are diagrammed in Figure 1A. Constructs were built to include a Kozak sequence and the LRP6 signal peptide upstream of the inserts, with two hemagglutinin (HA) tags in tandem added to the C-terminus.

The FLAG-MESD murine expression clone was the kind gift of B. Holdener. This plasmid was used as the template to create bacterial expression constructs and the C171A mutant by site-directed mutagenesis. For flow cytometry studies, the internal fragments of MESD were amplified by PCR and subcloned into pcDNA3 (Invitrogen) behind the MESD signal peptide and an N-terminal FLAG tag placed just after the signal peptidase cleavage site.

Biochemical Studies of Recombinant Mouse MESD. The mature mouse MESD cDNA was subcloned into a modified form of the vector pET15 (Novagen) with a His_6 tag followed by a tobacco etch virus cleavage site. The resulting expression plasmid was named pET15-MESD. Recombinant MESD was expressed in BL21 DE3 cells (Novagen) transformed with pET15-MESD by induction with 0.4 mM isopropyl β-D-thiogalactopyranoside (IPTG) for 3 h. Bacterial pellets were lysed by sonication in 50 mM Tris, pH 8.0, and 300 mM NaCl, and the lysate was captured onto Ni-NTA beads (Qiagen). After being washed with the same buffer, the protein was eluted from the beads with 50 mM imidazole and cleaved with His_6-TEV protease for 4 h at 30 °C. Cleaved fractions were reincubated with Ni-NTA beads to remove His_6-TEV, dialyzed against 50 mM Tris, pH 8.5, containing 10 mM NaCl and 1 mM DTT. The protein was then purified to apparent homogeneity by ion-exchange chromatography using a MonoQ HR 10/10 column (Pharmacia) on an AKTA system (Pharmacia).

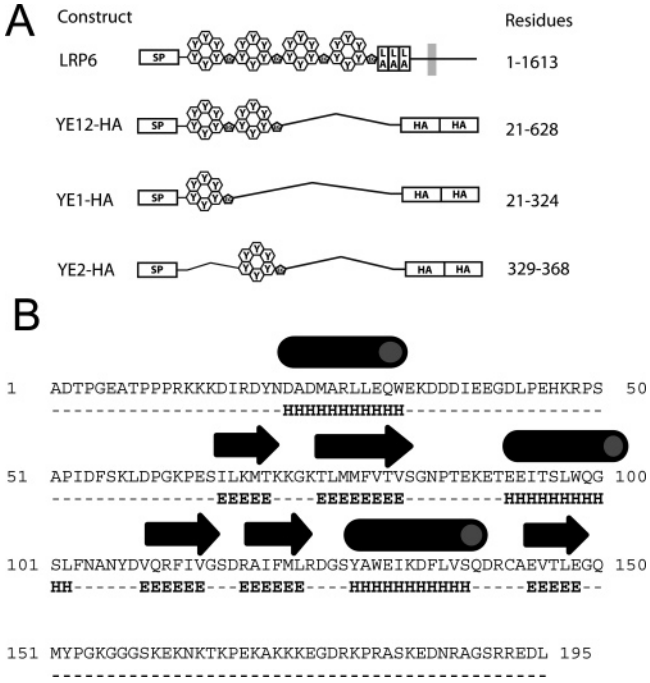

FIGURE 1: Schematic illustrating the predicted domain organizations of LRP6 and MESD. (A) Domain arrangement of native LRP6 and of the secreted minireceptors investigated in this study. Residues included within each construct are shown on the right. A pair of HA eptiope tags has been added at the C-terminal end of each secreted construct. (B) Predicted secondary structure organization of mouse MESD from the JPred structure prediction server (*15*). Cylinders above the sequence indicate sites of predicted helices, and arrows indicate sites of predicted β-strands.

(A) Gel Filtration. Purified MESD was concentrated to 2 mg/mL (90 μM), and 1 mL was injected onto a Superdex 75 HiLoad 16/60 gel filtration column (Pharmacia) on an FPLC system with a UV-2 detector. The buffer used was 20 mM Tris, pH 8.0, 150 mM NaCl, and 1 mM DTT, with a flow rate of 1 mL/min. Molecular weight standards were injected onto the column, and elution volumes were plotted as a function of the logarithm of the molecular weight to create a calibration curve.

(B) Limited Proteolysis Studies. Purified MESD (20 μg) was incubated with five serial dilutions of trypsin, V8 protease, and proteinase K (Boeringer Mannheim). Protease (2 μg) was used in the first cleavage reaction of the dilution series, and each successive dilution used 10-fold less protease. Reactions were carried out in 50 mM Tris, pH 8.0, 150 mM NaCl, 5 mM $CaCl_2$, and 1 mM DTT for 1 h at 37 °C. Reactions were quenched by the addition of hot 2× SDS−PAGE loading buffer and were analyzed by SDS−PAGE.

(C) Circular Dichroism Studies. CD scans were acquired on an AVIV 62DS spectropolarimeter, equipped with a Peltier effect temperature controller. MESD samples (20 μM) for CD were dialyzed into 20 mM sodium phosphate, pH 7.0, 20 mM NaCl, and 100 μM DTT. Scans were acquired from 196 to 260 nm, with a bandwidth of 1.5 nm, a scan step of 1 nm, an averaging time of 5 s, and five repeats per scan in a 1 mm path length cuvette. For thermal denaturation experiments, the temperature dependence of the molar ellipticity was followed at 217 and 222 nm. For thermal

denaturation studies, the temperature was raised 1 °C/min, using a bandwidth of 1.5 nm, an averaging time of 30 s, and an equilibration time of 2 min. CD wavelength scans obtained before and after thermal denaturation suggested a recovery of ~90% of the initial signal after conclusion of the thermal melt.

Cloning of Human FLAG-MESD. Full-length human MESD was amplified by PCR from a HUVEC cDNA library (a gift from G. Garcia-Cardena), using primers designed to amplify the sequence of the deposited gene (ID BC009210). Additional rounds of anchored PCR were done to extend the 5′ end and to include the MESD signal sequence, an internal FLAG epitope just after the predicted signal peptidase site, and flanking restriction sites to facilitate cloning into pcDNA3. The identity of the resulting clone (FLAG-HMesd) was verified by DNA sequencing.

Design of siRNA against Human MESD. To create siRNA oligonucleotides that knock down expression of human MESD, but not mouse MESD, the Invitrogen Block-It server and an alignment of human and mouse MESD coding sequences were used to design siRNA oligos directed against those parts of the MESD gene sequence that exhibit significant divergence between the human and mouse orthologues. The two oligos chosen were perfectly matched to the human sequence but possess between two and three nucleotide mismatches when compared to the mouse sequence (Figure S2).

Plasmid Transfections and Preparation of Conditioned Media and Whole Cell Lysates. HEK293T cells were cultured in DMEM (Invitrogen) supplemented with 10% FBS (Invitrogen) and 2 mM L-glutamine (Invitrogen). Cells were grown at 37 °C under 5% CO_2. On the day before transfection, HEK293T cells were seeded into 24-well dishes, at a confluency of 30%. On the day of transfection, cells were visually inspected to verify that the confluency was ~50%. Cells were then transfected with plasmid DNA using Lipofectamine 2000 (Invitrogen), according to the manufacturer's instructions. After 24 h, the culture media were collected into microfuge tubes and centrifuged for 5 min at 5000 rpm in a table-top microfuge to pellet any detached cells. The supernatant was transferred to a fresh tube for subsequent analysis. The cells in each well were mechanically detached in 500 μL of cold PBS, transferred to microfuge tubes, and recovered by centrifugation for 5 min at 5000 rpm in a table-top microfuge. After the supernatant was removed by aspiration, the cell pellet was resuspended in 200 μL of TBS containing 0.1% NP-40 and placed on ice for 30 min. The samples were then centrifuged at 13000 rpm for 5 min in a table-top microfuge, and the lysates were transferred to fresh tubes and stored at −80 °C until analysis.

siRNA Transfection in Propeller−EGF Domain Secretion Assays. Single wells containing HEK293T cells at 90% confluency were each transfected with siRNA, scrambled control siRNA, and a control siRNA against luciferase or were mock-transfected according to manufacturer's instructions. Five hours later, cells from each well were split at a confluency of 30% into 12 wells of a 24-well dish. The next day, each set of 12 wells were retransfected with the same siRNA reagents and allowed to incubate for 48 h. At 48 h, cells were transfected with plasmid DNA for different propeller−EGF domains and MESD constructs. Twenty-four hours later, conditioned media and whole cell lysates were prepared for analysis by SDS−PAGE followed by Western blotting.

Plasmid Transfection for β-Catenin Lucifersae Reporter Assay. HEK293T cells were transfected with siRNA oligonucleotides and controls as described in the above section. The resulting 12 wells in a 24-well dish were used to transfect cells with the β-catenin-responsive firefly luciferase construct TOPFLASH (*14*) and an internal control Renilla luciferase reporter plasmid. In addition, cells were transfected with plasmids encoding LRP, human Fz5, and human Wnt1 or all three plasmids together. Total DNA transfected per well was made up to 1 μg using pcDNA3. The four conditions were assayed in triplicate. Normalized firefly luciferase levels were measured in whole cell extracts 24 h after transfection using the dual luciferase kit (Promega) on a dual-channel luminometer (Turner Systems).

Preparation of siRNA Experiments for Analysis by FACS. HEK293T cells cultured in DMEM (Invitrogen) supplemented with 10% FBS (Invitrogen) and 2 mM glutamine were split into six-well dishes at a confluency of 50%. The next day, cells were visually inspected to verify that confluency was at 90%. Single wells were each transfected with siRNA oligos and control scrambled siRNA oligos or were mock transfected. Five hours after transfection, each well of transfected cells was split into three wells. Two days later, each set of three wells was visually inspected to verify that cell confluency was ~90%, and the cells were retransfected with the siRNA, control scrambled siRNA, or the mock condition, respectively. Five hours later, the cells were pooled and split into 24-well dishes at 40% confluency. The entire procedure yields three groups of cells: a mock-treated pool and two pools of cells treated with siRNA and a scrambled siRNA control, respectively.

The next day, the three pools of cells were transfected with VSV-G-tagged full-length LRP6, a cytoplasmic GFP (pEGFP1, Clontech) to mark transfected cells, and various forms of MESD. After 36 h, the supernatant media were aspirated, cells were washed by detaching them from each well in 500 μL of ice-cold PBS, and they were then transferred into an Eppendorf tube. Cells were pelleted at 5000 rpm for 5 min using a table-top microfuge and then resuspended in 200 μL of primary anti-VSV-G antibody solution and incubated on a rotator at 4 °C for 1 h. Cells were then recovered by centrifugation, washed once in PBS supplemented with 0.01% sodium azide, and resuspended in 200 μL of APC-conjugated secondary antibody solution and incubated on a rotator in the dark at 4 °C for 1 h. Primary antibody solution was a polyclonal rabbit anti-VSV-G antibody (Bethyl Labs) diluted 1:500 in PBS with 1% BSA and 0.1% sodium azide. Secondary antibody solution was an APC-conjugated goat anti-rabbit antibody (Molecular Probes) diluted 1:500 in PBS with 1% BSA and 0.1% sodium azide. For flow cytometric analysis, the cells were pelleted, washed in ice-cold PBS with azide, and transferred into 5 mL culture tubes (Falcon 2093) and placed on ice. To restrict analysis to transfected cells, a double gating strategy was set up as follows: Scattering properties were used to gate on live cells, followed by careful selection of GFP-positive cells to enrich for cells transfected with LRP6 and MESD. Using 10000 cells, a histogram plot was generated for each experimental condition. All data were acquired on

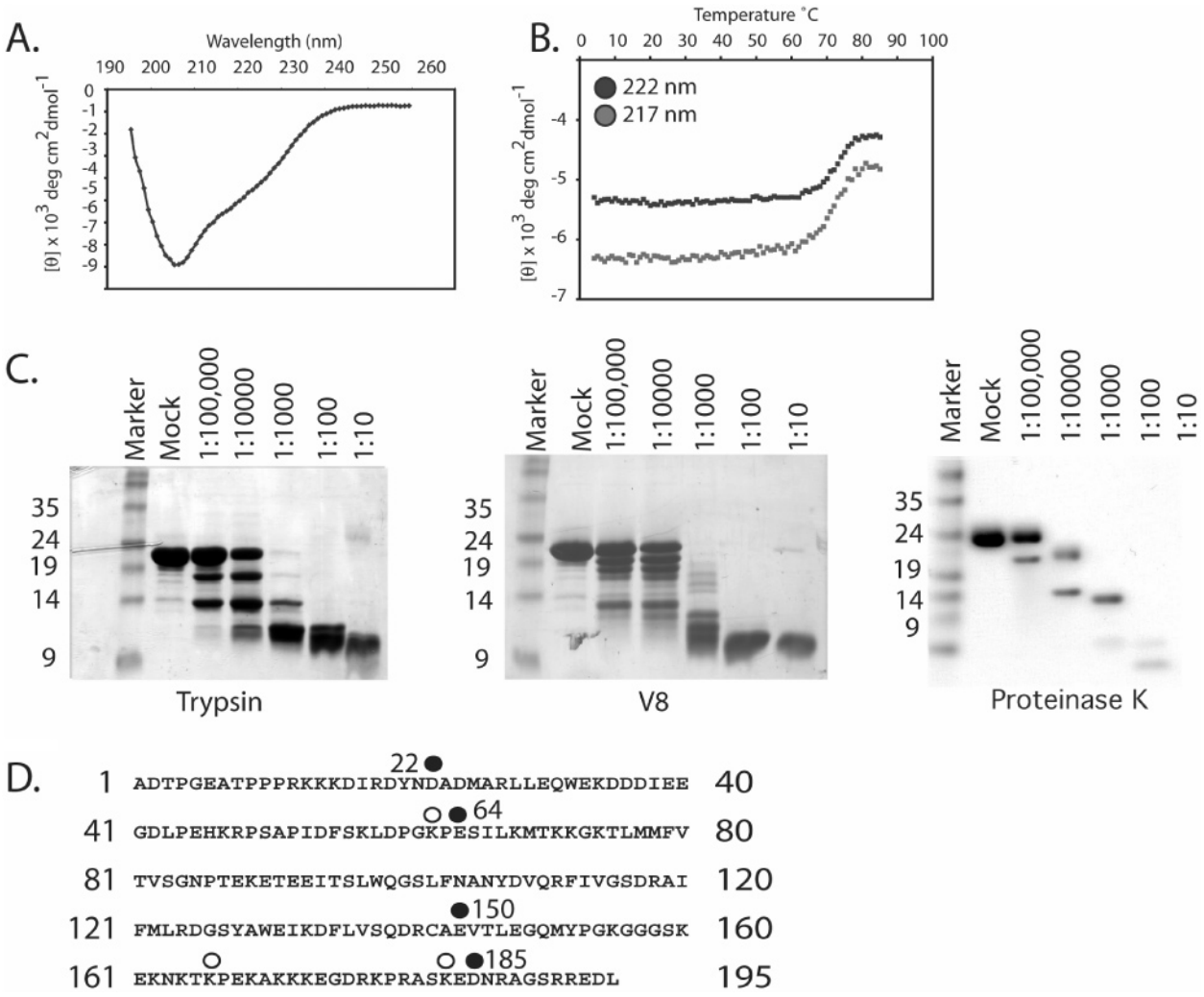

FIGURE 2: Biochemical evaluation of mouse MESD. (A) Circular dichroism scan plotting molar ellipticity of MESD as a function of wavelength. (B) Cooperative unfolding of MESD. The molar ellipticity of MESD at 217 nm (gray) and 222 nm (black) is plotted as a function of temperature during thermal denaturation. (C) Sensitivity of mouse MESD to limited proteolysis with trypsin (left panel), V8 protease (center panel), and proteinase K (right panel). Note the accumulation of a band of approximately 9 kDa that accumulates upon digestion with high concentrations of both trypsin and V8 protease and the accumulation of a proteinase K-resistant band of similar molecular mass at intermediate protease concentrations. (D) Sites of V8 (black dots) and trypsin (open dots) cleavage mapped onto the sequence of mature MESD.

a FACScalibur apparatus (BD Biosciences) and analyzed using the CellQuest Pro software (version 5.1.1).

RESULTS

MESD Contains a Central Structured Region Flanked by Flexible N- and C-Termini. The Jpred server (*15*, *16*) predicts that mouse MESD contains a core domain (residues 66−148 of the mature protein, which correspond to residues 95−177 of the encoded polypeptide) that is predominantly β in structure. Otherwise, the N- and C-terminal sequences are predicted to adopt a random coil conformation, with the exception of an isolated predicted helix within the N-terminal region from residues 22−32 (Figure 1B). In toto, 50% of the sequence is predicted to be unstructured, consistent with output from the PONDR algorithm, which predicts that the MESD sequence is at least 53% disordered (*17*).

MESD is readily expressed as a recombinant protein in bacteria and elutes at a volume consistent with its monomeric molecular weight from an S75 gel filtration column (Figure S1). The far-UV CD spectrum of MESD shows a broad minimum at 208 nm, with the shape of the spectrum most consistent with a mixture of β structure and random coil (Figure 2A). The temperature dependence of the molar ellipticity signal at wavelengths characteristic of secondary structural elements (217 and 222 nm) displays a cooperative transition at 80 °C (Figure 2B), consistent with the unfolding of a stable, core folded domain.

To identify a part of MESD corresponding to a proteolytically resistant folded core, we subjected MESD to limited proteolysis using substoichiometric amounts of the enzymes trypsin, V8 protease, and proteinase K (Figure 2C). Persistent fragments following proteolysis were analyzed by MALDI-TOF mass spectrometry, and predicted fragment boundaries were mapped onto the sequence of MESD (Figure 2D). The majority of potential trypsin and V8 protease cleavage sites are highly protected within a core region spanning residues 64−150, indicating that this part of the protein represents a core, folded domain. The sites of proteolytic cleavage were used as landmarks for the design of internal fragments of MESD used to probe function in subsequent experiments (see below).

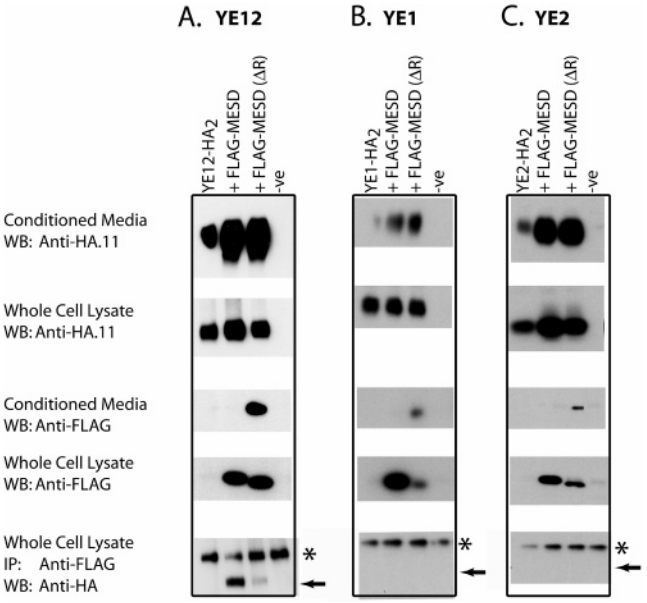

FIGURE 3: Coexpression of MESD enhances secretion of LRP6 minireceptors. (A) Enhancement of YE12 secretion by cotransfection with ER-retained and secreted forms of MESD. Note also the co-immunoprecipitation of YE12 with FLAG-MESD in the bottom panel. (B, C) Enhancement of YE1 secretion (B) and YE2 secretion (C) by cotransfection with MESD. In each panel LRP6 minireceptors were detected by Western blot for the HA epitope tag, and MESD proteins were detected by blotting for the FLAG epitope tag. The signal resulting from reactivity of the immunoglobulin heavy chain is indicated with an asterisk.

MESD Enhances Secretion of Human LRP6 Subdomains Containing One or Two Propeller−EGF Domain Pairs. Enforced expression studies reported elsewhere have shown that coexpression of MESD enhances surface expression of epitope-tagged LRP6. Previous studies of Boca in flies also indicated that Boca can promote productive maturation of even a single YWTD-EGF domain pair (*11*). To map the minimum-length fragment of LRP6 responsive to MESD coexpression and test whether MESD analogously enhances productive maturation of LRP6-derived minireceptors containing one or two YWTD-EGF domain pairs (Figure 1A), we investigated the effect of MESD coexpression on the secretion of different minireceptors containing one or two YWTD-EGF units (Figure 3). We chose to focus on the first two propellers of LRP6 because of the known disease-associated mutations in the first propeller of LRP5 and the reported effects of these mutations on association of LRP5 with MESD (*12*). Secretion of YE12 (Figure 3A), YE1 (Figure 3B), and YE2 (Figure 3C) from transfected cells is enhanced by cotransfection of murine MESD, consistent with the near global effect of Boca on the secretion of single propeller−EGF pairs derived from Arrow and other LRPs and with another report assessing the influence of MESD on secretion of the single YE12 fragment of human LRP5 (*12*).

MESD Coprecipitates with YE12 but Not with YE1 or YE2 Alone. We next tested whether any of the LRP6-derived minireceptors co-immunoprecipitated with FLAG-tagged murine MESD (FLAG-MESD) or with FLAG-tagged murine MESD without a C-terminal ER retention signal. Whole cell lysates from cells cotransfected with various HA-tagged propeller−EGF constructs and murine FLAG-MESD were incubated with anti-FLAG beads, and the recovery of the

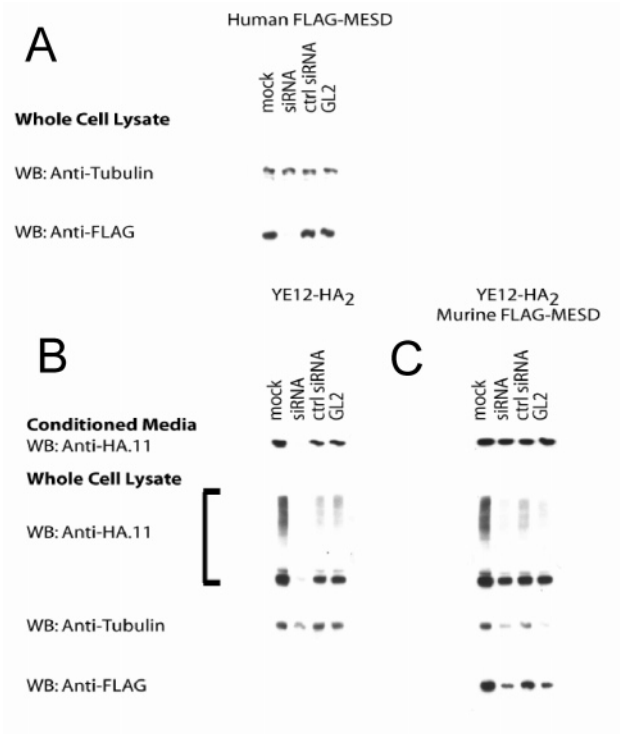

FIGURE 4: Inhibition of minireceptor secretion by siRNA directed against human MESD. (A) siRNA against human MESD suppresses expression of cotransfected FLAG-tagged human MESD. (B) Effect of siRNA directed against human MESD. Secretion of YE12 into the conditioned media is suppressed (upper panel), and the protein does not accumulate to detectable levels intracellularly (bottom panel), based on Western blot detection of the HA epitope. (C) Rescue by mouse MESD. YE12 is secreted into the conditioned media (top panel) and accumulates to detectable steady-state levels intracellularly (bottom panel), based on Western blot detection of the HA epitope. The mouse MESD is resistant to the siRNA against human MESD (bottom panel).

various LRP6 minireceptors was assessed by Western blot (Figure 3, bottom panels). Whereas the YE12 minireceptor coprecipitates with FLAG-MESD, YE1 and YE2 do not. This observation is consistent with a previous report that YE12 from LRP5 also coprecipitates with MESD (*12*).

Cloning and Functional Analysis of Human MESD. To examine the influence of MESD loss of function on LRP6 maturation using an siRNA approach (Figure 4), we cloned the human MESD gene and exploited differences in the human and murine coding sequences to design two siRNA oligos (siRNA 1 and siRNA 2) selective for knockdown of human but not mouse MESD (Figure S2). siRNA 1 effectively knocks down expression of FLAG-MESD (Figures S2 and 4A), whereas expression of murine FLAG-MESD is resistant to knockdown by siRNA 1 (Figures S2 and Figure 4C, bottom panel). Therefore, we used this siRNA (henceforth designated "siRNA") to examine the effect of depleting endogenous MESD on minireceptor secretion and on full-length LRP6 maturation, using rescue by murine MESD to confirm the specificity of the knockdown effect.

MESD Is Required for the Secretion and Intracellular Survival of YE12. To test whether endogenous MESD is needed for secretion of transfected YE12, we treated cells with control siRNA or siRNA against MESD and analyzed the conditioned media of the cultured cells by Western blot (Figure 4). In mock-transfected cells and cells treated with

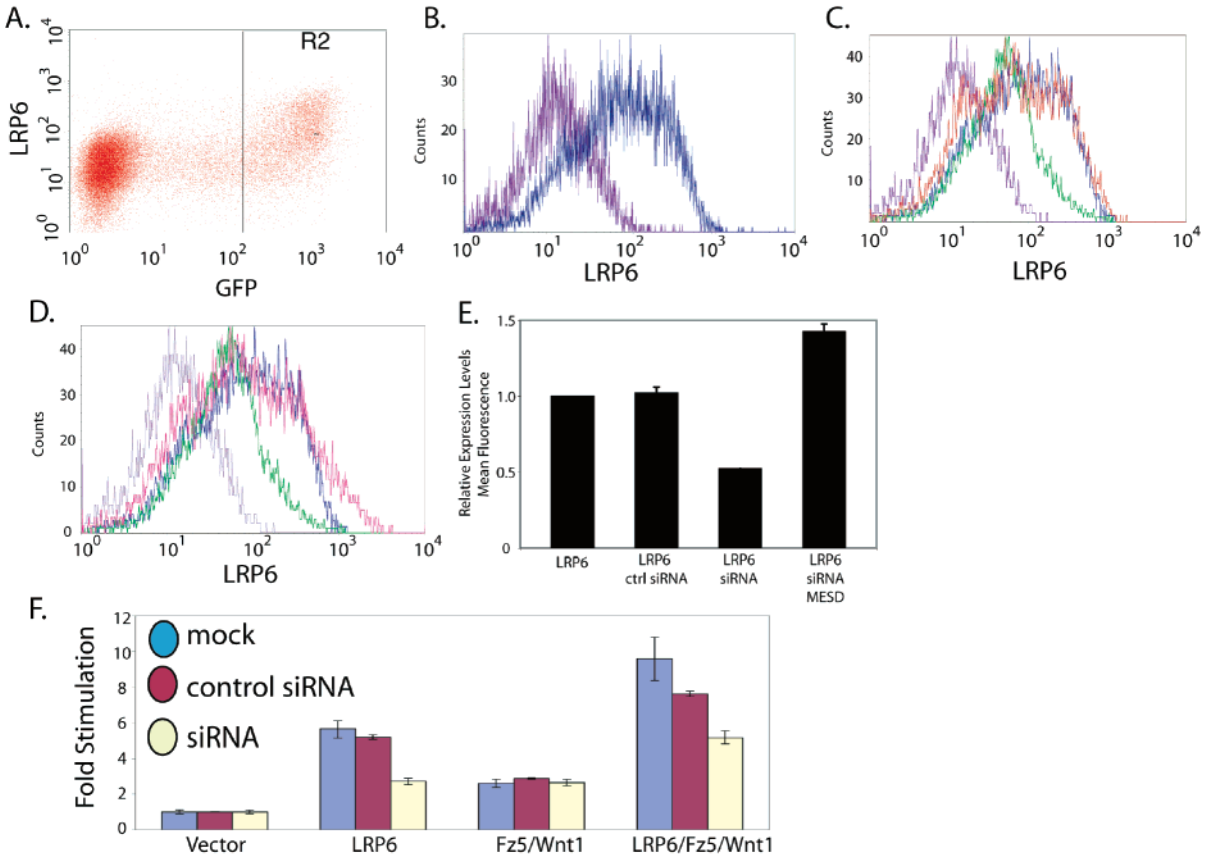

FIGURE 5: Role of MESD in maturation of cell-surface LRP6. (A) Cell population selected for subsequent analysis. The GFP signal is on the *X*-axis, and the LRP6 expression level is plotted on the *Y*-axis. (B) Flow cytometry plot illustrating VSV-tagged LRP6 surface expression after gating on GFP-positive cells (blue, 293T cells transfected with plasmids expressing GFP and VSV-LRP6; purple, 293T cells transfected with plasmids expressing GFP and empty vector). (C) Reduction in cell-surface LRP6 upon siRNA knockdown of human MESD. Key: purple, no LRP6; blue, LRP6; red, LRP6 plus control siRNA; green, LRP6 plus siRNA. (D) Rescue of siRNA-mediated knockdown of human MESD by cotransfection with mouse MESD. Key: light purple, no LRP6; blue, LRP6; green, LRP6 plus siRNA; red, LRP6 plus mouse MESD (M). (E) Bar graphs quantifying the mean fluorescence from detection of surface VSV-G-tagged LRP6 after MESD knockdown and rescue in the flow cytometry experiments. The error bars indicate standard deviation of the VSV-G epitope signal. (F) Luciferase reporter assay (see Materials and Methods). Addition of siRNA against human MESD inhibits LRP-dependent Wnt signaling. Key: blue bars, mock siRNA; red bars, control siRNA; yellow bars, siRNA directed against human MESD.

scrambled or luciferase-targeted siRNA controls, the secretion of YE12 was not affected. In contrast, cells receiving the siRNA directed against human MESD exhibit a dramatic reduction in the amount of minireceptor secreted into the media (Figure 4B, top panel). Examination of the whole cell lysate also shows that treatment of cells with siRNA leads to a decrease in steady-state intracellular YE12 (Figure 4B, middle panel). The effect of knockdown on both secretion and intracellular minireceptor accumulation is specific for loss of MESD, because cotransfection of murine MESD fully rescues both the protein accumulation and secretion defects (Figure 4C). Taken together, these data show that MESD is needed to promote passage of these LRP6 minireceptors through the secretory pathway and suggest that MESD enhances the resistance of nascent minireceptors to degradation, perhaps by promoting proper folding.

MESD Promotes Cell-Surface Expression of LRP6. To extend the findings from our minireceptor studies to full-length LRP6, we used flow cytometry to quantify the effects of siRNA knockdown of endogenous MESD on the cell-surface expression of LRP6 (Figure 5). When 293T cells are transfected with VSV-tagged LRP6, the amount of protein on the surface of the transfected cells at steady state (transfection efficiency ~25%; Figure 5A) can be readily quantified by flow cytometry (Figure 5B). Treatment of the cells with the siRNA against human MESD leads to a 2-fold drop in the mean fluorescence signal in the transfected cell population (Figure 5C), which is fully rescued upon cotransfection with murine MESD (Figure 5D,E). In fact, the mean expression level in the cells rescued with murine MESD exhibits a significant and reproducible increase above the level seen in cells treated with LRP6 alone (Figure 5D,E). These findings complement previous reports showing that enforced expression of MESD enhances cell-surface delivery of full-length LRP6 (*10*) and secretion of an LRP5 minireceptor (*12*) and provide convincing evidence that MESD is indeed required for efficient maturation and cell-surface expression of LRP6.

Effect of MESD Knockdown on Wnt Signal Transduction. We next examined whether MESD knockdown had an effect on the function of LRP6 as a Wnt coreceptor by assaying β-catenin-dependent transcription of a luciferase reporter gene under various treatment conditions. As predicted on the basis of the surface expression studies, MESD knockdown leads to a ~50% reduction in luciferase activity in cells transfected with either LRP6 or a combination of LRP6, Wnt1, and Frizzled 5 (Figure 5E).

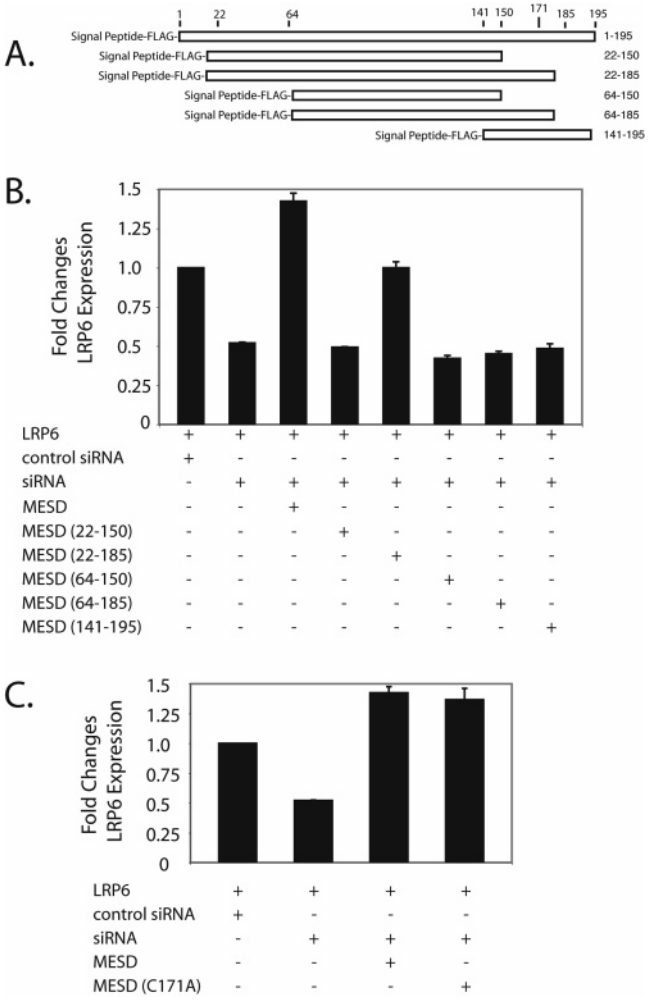

FIGURE 6: Mapping regions of MESD required for function. (A) Mouse MESD constructs tested for rescue of siRNA-mediated knockdown of human MESD. (B) Bar graphs quantifying the mean fluorescence from detection of VSV-G-tagged surface LRP6 after MESD knockdown and rescue with various MESD constructs in flow cytometry experiments. The error bars indicate standard deviation of the VSV-G epitope signal. Only MESD 22−185 rescues surface LRP6 expression after siRNA knockdown. (C) MESD is not a redox catalyst. Bar graphs comparing rescue of siRNA-mediated knockdown of human MESD by wild-type and the C171A form of mouse MESD.

Mapping Experiments. To map a minimum-length fragment of MESD that still promotes LRP6 transport to the cell surface, we also tested a series of overlapping deletion constructs of murine MESD for their ability to rescue cell-surface expression of VSV-tagged LRP6 following knockdown of endogenous human MESD in the flow cytometry assay. The MESD deletion proteins were designed on the basis of the results of the limited proteolysis experiments (Figures 2D and 6A). Of five constructs tested, only MESD 22−185 exhibited rescue of the surface expression defect, implicating N-terminal residues between positions 22−64 and C-terminal residues between positions 150−185 as important for MESD function (Figure 6B). In agreement with our findings, others have reported that deletion of residues 150−195 from murine MESD also reduces surface expression of LRP6 in a cotransfection assay (*18*). The Boca mutation W49R, which is conserved in MESD and lies within the N-terminal deleted region of these studies, also acts as a loss-of-function mutation (*9*), again consistent with the findings reported here.

MESD Is Not a Redox Catalyst. Hsieh et al. (*10*) reported that cotransfection of MESD with LRP6 reduces the fraction of protein that forms disulfide-linked aggregates and improves the fraction of protein that migrates at the predicted monomeric molecular weight in nonreducing gels. Because MESD possesses a single unpaired cysteine (C171), we tested the hypothesis that MESD acts as a redox catalyst to facilitate LRP6 folding by examining the ability of the C171A mutant of murine MESD to rescue cell-surface expression of VSV-tagged LRP6 following knockdown of endogenous human MESD in the flow cytometry assay. Thus, we compared the ability of normal murine and MESD (C171A) to rescue defects in LRP6 surface expression caused by siRNA-mediated knockdown of endogenous MESD. The reduced expression of LRP6 seen in cells depleted of human MESD by siRNA knockdown is equally rescued by both normal and C171A FLAG-MESD, providing strong evidence that cysteine 171 is not required for MESD to promote LRP6 cell-surface expression and arguing that MESD is not a redox catalyst (Figure 6C). By extension, the role of MESD in reducing intramolecular disulfide-bonded aggregates is likely to be indirect, though other interacting ER-resident proteins and the identification of these binding partners are important future goals.

DISCUSSION

These studies investigate the role of the mammalian protein MESD in promoting transit of the LDL receptor-related protein 6 (LRP6) to the cell surface. MESD is an ER-resident protein previously implicated in LRP6 maturation based on the phenotype of the MESD knockout mouse and enforced expression studies in mammalian cells. Here, we establish that loss of MESD resulting from siRNA treatment prevents secretion of LRP6 minireceptors into the cell culture media and markedly reduces the amount of full-length LRP6 that reaches the cell surface.

How does MESD facilitate transit of LRP6 and other LDL receptor-related proteins to the cell surface? The most likely possibility is that MESD is a catalyst for folding of the propeller domains of LDL receptor family proteins, either by directly promoting the acquisition of the native fold or by preventing aggregation. In this model, successful interaction with MESD leads to productive folding and subsequent maturation of propeller−EGF units, but when MESD is not present, misfolded or unfolded chains are targeted for degradation by ERAD. This model is consistent with our MESD knockdown studies, in which reduced endogenous MESD expression leads to a decrease in intracellular steady-state levels of YE12 (Figure 4) and in the surface expression of full-length LRP6 (Figures 5 and 6). If MESD is a catalyst of the folding step, however, it is not acting directly as a redox catalyst because the C171A mutant still supports maturation of both minireceptors and full-length LRP6. An alternative possibility for the role of MESD in promoting receptor maturation is that it transfers natively folded propeller−EGF domains from the ER into the cis-Golgi.

Given that natively disordered regions of MESD are required for its function as a maturation factor for LDLR family proteins, it is especially interesting that intrinsically disordered regions are required for the function of other

protein chaperones like Hsp25 family members (*19*) and the p23 cofactor of Hsp90 family chaperones (*20*). Furthermore, PONDR analysis of a large group of different protein chaperones, including various Hsp family members, reveals that nearly 40% of the residues fall into disordered regions (*21*). Disordered regions within protein chaperones confer three distinct advantages to substrate recognition. First, because unfolded regions of the protein possess disproportionately large intermolecular interfaces and can explore a larger conformational space (*22*), they can recognize a larger number of substrates with a broader range of substrate conformations. Second, because unfolded polypeptides are not tightly constrained by stabilizing interactions, they can explore conformational space and bind to potential partners more quickly (*23*). Finally, binding to substrate often leads to ordering or folding of the chaperone sequence; the released energy can be used to enhance substrate folding.

These advantages may be important for the chaperone activity of MESD/Boca on propeller−EGF domains of different lipoprotein receptors. Multiple sequence alignments of propeller−EGF domains from different receptors reveal that the average sequence identity between members is only ∼25%. Furthermore, despite significant predicted structural homology (*24*, *25*), individual domains are functionally distinct. For example, while the second propeller−EGF domain of LRP6 can functionally substitute for the propeller−EGF domain of the LDLR, the fourth propeller−EGF domain cannot (*26*). Taken together, these data suggest that propeller−EGF domains possess significant sequence and functional diversity. The natively unfolded character of the N- and C-termini of MESD and, by extension, Boca may be of great help in their roles as private chaperones to this diverse group of substrates.

ACKNOWLEDGMENT

We thank Kristine Estrada for digestion of MESD with proteinase K and are grateful to members of the Blacklow laboratory, Dr. Xi He, and Dr. Jon Aster for thoughtful discussions.

SUPPORTING INFORMATION AVAILABLE

Figures S1 and S2 as described in the text. This material is available free of charge via the Internet at http://pubs.acs.org.

REFERENCES

1. Nusse, R. (2005) Wnt signaling in disease and in development, *Cell Res. 15*, 28−32.
2. Pinson, K. I., Brennan, J., Monkley, S., Avery, B. J., and Skarnes, W. C. (2000) An LDL-receptor-related protein mediates Wnt signalling in mice, *Nature 407*, 535−538.
3. Wehrli, M., Dougan, S. T., Caldwell, K., O'Keefe, L., Schwartz, S., Vaizel-Ohayon, D., Schejter, E., Tomlinson, A., and DiNardo, S. (2000) Arrow encodes an LDL-receptor-related protein essential for Wingless signalling, *Nature 407*, 527−530.
4. Tamai, K., Semenov, M., Kato, Y., Spokony, R., Liu, C., Katsuyama, Y., Hess, F., Saint-Jeannet, J. P., and He, X. (2000) LDL-receptor-related proteins in Wnt signal transduction, *Nature 407*, 530−535.
5. Cong, F., Schweizer, L., and Varmus, H. (2004) Wnt signals across the plasma membrane to activate the beta-catenin pathway by forming oligomers containing its receptors, Frizzled and LRP, *Development 131*, 5103−5115.
6. Brown, S. D., Twells, R. C., Hey, P. J., Cox, R. D., Levy, E. R., Soderman, A. R., Metzker, M. L., Caskey, C. T., Todd, J. A., and Hess, J. F. (1998) Isolation and characterization of LRP6, a novel member of the low density lipoprotein receptor gene family, *Biochem. Biophys. Res. Commun. 248*, 879−888.
7. Mao, B., Wu, W., Li, Y., Hoppe, D., Stannek, P., Glinka, A., and Niehrs, C. (2001) LDL-receptor-related protein 6 is a receptor for Dickkopf proteins, *Nature 411*, 321−325.
8. Semenov, M. V., Tamai, K., Brott, B. K., Kuhl, M., Sokol, S., and He, X. (2001) Head inducer Dickkopf-1 is a ligand for Wnt coreceptor LRP6, *Curr. Biol. 11*, 951−961.
9. Culi, J., and Mann, R. S. (2003) Boca, an endoplasmic reticulum protein required for wingless signaling and trafficking of LDL receptor family members in *Drosophila*, *Cell 112*, 343−354.
10. Hsieh, J. C., Lee, L., Zhang, L., Wefer, S., Brown, K., DeRossi, C., Wines, M. E., Rosenquist, T., and Holdener, B. C. (2003) Mesd encodes an LRP5/6 chaperone essential for specification of mouse embryonic polarity, *Cell 112*, 355−367.
11. Culi, J., Springer, T. A., and Mann, R. S. (2004) Boca-dependent maturation of beta-propeller/EGF modules in low-density lipoprotein receptor proteins, *EMBO J. 23*, 1372−1380.
12. Zhang, Y., Wang, Y., Li, X., Zhang, J., Mao, J., Li, Z., Zheng, J., Li, L., Harris, S., and Wu, D. (2004) The LRP5 high-bone-mass G171V mutation disrupts LRP5 interaction with Mesd, *Mol. Cell. Biol. 24*, 4677−4684.
13. Chenna, R., Sugawara, H., Koike, T., Lopez, R., Gibson, T. J., Higgins, D. G., and Thompson, J. D. (2003) Multiple sequence alignment with the Clustal series of programs, *Nucleic Acids Res. 31*, 3497−3500.
14. Korinek, V., Barker, N., Morin, P. J., van Wichen, D., de Weger, R., Kinzler, K. W., Vogelstein, B., and Clevers, H. (1997) Constitutive transcriptional activation by a beta-catenin-Tcf complex in APC−/− colon carcinoma, *Science 275*, 1784−1787.
15. Cuff, J. A., and Barton, G. J. (2000) Application of multiple sequence alignment profiles to improve protein secondary structure prediction, *Proteins 40*, 502−511.
16. Cuff, J. A., Clamp, M. E., Siddiqui, A. S., Finlay, M., and Barton, G. J. (1998) JPred: a consensus secondary structure prediction server, *Bioinformatics 14*, 892−893.
17. Iakoucheva, L. M., Brown, C. J., Lawson, J. D., Obradovic, Z., and Dunker, A. K. (2002) Intrinsic disorder in cell-signaling and cancer-associated proteins, *J. Mol. Biol. 323*, 573−584.
18. Li, Y., Chen, J., Lu, W., McCormick, L. M., Wang, J., and Bu, G. (2005) Mesd binds to mature LDL-receptor-related protein-6 and antagonizes ligand binding, *J. Cell Sci. 118*, 5305−5314.
19. Lindner, R. A., Carver, J. A., Ehrnsperger, M., Buchner, J., Esposito, G., Behlke, J., Lutsch, G., Kotlyarov, A., and Gaestel, M. (2000) Mouse Hsp25, a small shock protein. The role of its C-terminal extension in oligomerization and chaperone action, *Eur. J. Biochem. 267*, 1923−1932.
20. Weikl, T., Abelmann, K., and Buchner, J. (1999) An unstructured C-terminal region of the Hsp90 co-chaperone p23 is important for its chaperone function, *J. Mol. Biol. 293*, 685−691.
21. Tompa, P., and Csermely, P. (2004) The role of structural disorder in the function of RNA and protein chaperones, *FASEB J. 18*, 1169−1175.
22. Gunasekaran, K., Tsai, C. J., Kumar, S., Zanuy, D., and Nussinov, R. (2003) Extended disordered proteins: targeting function with less scaffold, *Trends Biochem. Sci. 28*, 81−85.
23. Shoemaker, B. A., Portman, J. J., and Wolynes, P. G. (2000) Speeding molecular recognition by using the folding funnel: the fly-casting mechanism, *Proc. Natl. Acad. Sci. U.S.A. 97*, 8868−8873.
24. Jeon, H., Meng, W., Takagi, J., Eck, M. J., Springer, T. A., and Blacklow, S. C. (2001) Implications for familial hypercholesterolemia from the structure of the LDL receptor YWTD-EGF domain pair, *Nat. Struct. Biol. 8*, 499−504.
25. Springer, T. A. (1998) An extracellular beta-propeller module predicted in lipoprotein and scavenger receptors, tyrosine kinases, epidermal growth factor precursor, and extracellular matrix components, *J. Mol. Biol. 283*, 837−862.
26. Beglova, N., Jeon, H., Fisher, C. and Blacklow, S. C. (2004) Cooperation of fixed and low pH-inducible interfaces controls lipoprotein release by the LDL receptor, *Mol. Cell 6*, 281−292.

BI700049G